

Unimodality of Wave Amplitude in the Northern Hemisphere

MAARTEN H. P. AMBAUM

Department of Meteorology, University of Reading, Reading, United Kingdom

(Manuscript received 19 September 2006, in final form 29 June 2007)

ABSTRACT

A novel statistic for local wave amplitude of the 500-hPa geopotential height field is introduced. The statistic uses a Hilbert transform to define a longitudinal wave envelope and dynamical latitude weighting to define the latitudes of interest. Here it is used to detect the existence, or otherwise, of multimodality in its distribution function. The empirical distribution function for the 1960–2000 period is close to a Weibull distribution with shape parameters between 2 and 3. There is substantial interdecadal variability but no apparent local multimodality or bimodality.

The zonally averaged wave amplitude, akin to the more usual wave amplitude index, is close to being normally distributed. This is consistent with the central limit theorem, which applies to the construction of the wave amplitude index. For the period 1960–70 it is found that there is apparent bimodality in this index. However, the different amplitudes are realized at different longitudes, so there is no bimodality at any single longitude.

As a corollary, it is found that many commonly used statistics to detect multimodality in atmospheric fields potentially satisfy the assumptions underlying the central limit theorem and therefore can only show approximately normal distributions. The author concludes that these techniques may therefore be suboptimal to detect any multimodality.

1. Introduction

The idea of multiple equilibria in the atmosphere was given prominence by the seminal work of Charney and DeVore (1979). This idea is attractive on many levels. It may explain the apparent occurrence of weather regimes. It would also mirror low-order nonlinear models that have been used as didactic analogs for more complex behavior in the real atmosphere.

Whether multiple equilibria actually exist in the atmosphere is as yet unclear. Authors have been showing statistical evidence of multiple equilibria for many years (e.g., Hansen and Sutera 1986; Mo and Ghil 1988; Kimoto and Ghil 1993; Corti et al. 1999; Monahan et al. 2001; Christiansen 2005a). However, almost with equal regularity others have pointed out a lack of statistical significance in these results (Nitsche et al. 1994; Stephenson et al. 2004; Christiansen 2005b). The problems have been confounded by parameter dependence of the statistics used and of the significance testing.

Whether the atmosphere has multiple equilibria appears to be more an article of faith than an observed reality.

The elegance of low-order nonlinear models as didactic analogs (e.g., Palmer 1999) has probably increased our desire to find multiple equilibria in the real atmosphere. However, these low-order models are by construction not realistic. The multiple equilibria in the Charney and DeVore (1979) model were found to occur in unrealistic parameter regimes (Tung and Rosenthal 1985). Other simple models of multiple equilibria focusing on nonlinear oscillators (e.g., Malguzzi and Speranza 1981) have always involved many idealizations, although, perhaps surprisingly, the multiple equilibria in the more realistic barotropic model of Ambaum and Verkley (1995) can be mapped on response curves of nonlinear oscillators (Ambaum 1997).

It may be argued (D. Straus 2006, personal communication; Stan and Straus 2007) that there is a distinction between weather regimes, as exemplified by Baur's Großwetterlagen, and circulation regimes, as measured, for example, by the Rossby and Namias index cycles. The latter are usually thought of as global nonlinear resonances while weather regimes, as experienced by the synoptician, may be bimodal or multimodal.

Corresponding author address: Dr. Maarten Ambaum, Department of Meteorology, University of Reading, P.O. Box 243, Reading RG6 6BB, United Kingdom.
E-mail: m.h.p.ambaum@reading.ac.uk

dal only quite locally in both time and space. It is then not clear that a long-term global statistic would usefully reflect the residence of the atmosphere in various weather regimes.

Theories underlying local weather regimes are inspired by the observed quasi-stationary nature of blocked flows and zonal flows. For example, modons (e.g., McWilliams 1980; Verkley 1984; Flierl 1987) are solutions of the equations of motion that represent local nonlinear perturbations of the flow with closed recirculation regions, thus representing different flow topology from a zonal background flow. Such flow structures can be sought in models (e.g., Branstator and Opsteegh 1989) or observations (e.g., Ek and Swaters 1994) by looking for regions with one-to-one relationships between the streamfunction and the potential vorticity, such that the flow is (quasi) stationary. More recently, Swanson (2002) has been reviewing how in simple models large local perturbations on jet streams can be formed. These studies suggest that localized nonlinear flow structures are dynamically possible and share many aspects with observed flow structures. Although the topological changes required for modonlike recirculations cannot formally be achieved by the adiabatic rearrangements in the simplified model of Swanson (2002), it does provide a convincing route to strong local perturbations by accumulation of wave activity.

In this paper we construct and analyze a local wave amplitude statistic that is largely nonparametric (section 2) and is not influenced by secular trends or decadal variability in jet location. It allows us to identify local wave amplitude anomalies that do not necessarily rely on global resonances. We find that there is no strong indication for bimodality or multimodality in the 500-hPa geopotential height amplitude (section 3) or the highly related wave amplitude index (WAI; Hansen and Sutera 1986). We also find that the bimodality observed in Hansen and Sutera's wave amplitude index is most likely not a reflection of true bimodality at any location, but rather an artifact of aliasing two different mean amplitudes at different longitudes into a single index (section 4). Integrated statistics, such as the wave amplitude index or principal component time series, are found to be suffering from the fast convergence to Gaussian statistics of the central limit theorem, which makes such indices suboptimal to detect potential bimodality.

2. Local wave amplitude

For any periodic function $f(x)$ we can define a local wave amplitude $A(x)$ as

$$A^2 = f^2 + (f^H)^2, \quad (1)$$

where f^H is the spatial Hilbert transform of f (e.g., von Storch and Zwiers 1999). The Hilbert transform is most easily defined in the spectral domain: the Fourier transform \hat{f} of f and its Hilbert transform \hat{f}^H are related through

$$\hat{f}^H = i \operatorname{sgn}(k) \hat{f}, \quad (2)$$

where k is the wavenumber. In other words, to find the Hilbert transform of a periodic function, each Fourier component is shifted by a quarter wavelength so that all sines become cosines and all cosines become negative sines. Additional properties of Hilbert transforms can be found in von Storch and Zwiers (1999). An application of the Hilbert transform in atmospheric dynamics can be found in Ambaum and Athanasiadis (2007), where it plays a central role in the dynamics of Rossby edge waves and where the wave amplitude, as defined above, was shown to be locally conserved for linearized surface quasigeostrophic dynamics. An application of the Hilbert transform to wave amplitude diagnostics can be found in Zimin et al. (2003).

The above definition of wave amplitude has some desirable properties that make it a natural choice. A monochromatic wave $A \cos(kx + \phi)$ is found to have a constant wave amplitude A . For superpositions of monochromatic waves the wave amplitude describes the wave envelope, as can be checked using simple test functions. For example, choose $f = \cos(k + \epsilon)x + \cos(k - \epsilon)x$. This can be rewritten as $f = 2 \cos kx \operatorname{cosex}$, and for $\epsilon \ll k$ it can be interpreted as a carrier wave of wavenumber k modulated with an amplitude of $2 \operatorname{cosex}$. The Hilbert transform of f is $f^H = -\sin(k + \epsilon)x - \sin(k - \epsilon)x$, and we find that $f^2 + (f^H)^2 = (2 \operatorname{cosex})^2$, as expected for $\epsilon \ll k$; when this criterion is not met, the current definition still provides the envelope of the full wave.

We will use this local wave amplitude definition to provide an amplitude measure for 500-hPa geopotential height anomalies as a function of longitude. The advantage of a longitude-dependent local amplitude above a zonally averaged measure, such as Hansen and Sutera's (1986) wave amplitude index, is that synoptic experience shows that most interesting large-scale waves have the form of localized blocks, usually over the Atlantic and Pacific basins. The local wave amplitude allows isolation of a consistent definition of wave amplitude over those areas. Another advantage is that our local wave amplitude is independent of the phase of the carrier wave under consideration. So, if the internal structure of the block (i.e., the phase of the carrier wave) moves slightly or the block evolves under incident mobile systems, the local wave amplitude remains con-

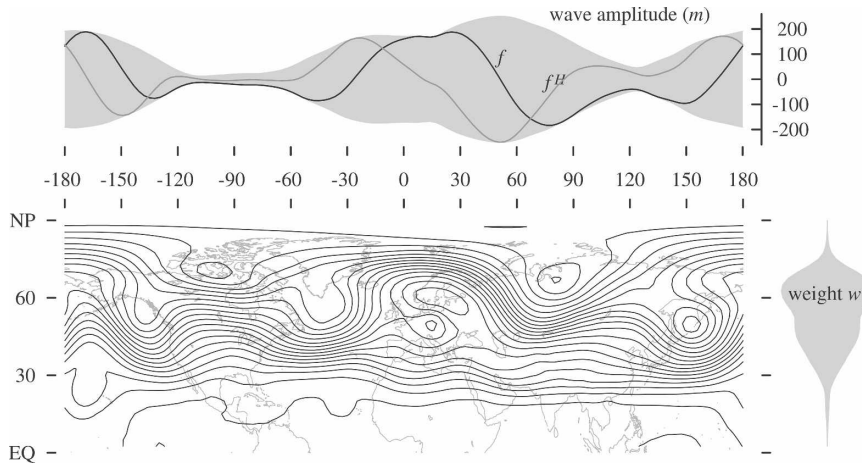


FIG. 1. Contour map of the low-pass filtered geopotential height at 500 hPa for 0000 UTC 7 February 1994 (contour interval, 50 m): (bottom right) weight as a function of latitude and (top) wave amplitude (shaded, in meters) as a function of longitude with the weighted geopotential anomaly f (black) and its Hilbert transform f^H (gray).

stant, contrary to measures dependent on prescribed patterns (such as, e.g., the North Atlantic Oscillation). This reflects the synoptic experience that the area under consideration is still experiencing high wave amplitude even though the exact phase might vary because of smaller-scale development. A third advantage is that the local wave amplitude does not contain parameters, so no spatial wavenumbers are chosen that could give rise to parameter dependency of its statistics.

The usual method to find a longitude-dependent measure of 500-hPa geopotential height variation is to average the field over a particular latitude belt. This has some obvious disadvantages. A good example may be the transition from a zonal flow to a strongly blocked flow. For the zonal flow the wave amplitude of interest is around the subtropical jet latitudes, while for the blocked flow the waves of interest are farther north, generally away from the zonal mean jet(s). To capture all cases we would need to choose a very wide latitude belt, which gives rise to washed-out statistics. If a narrower band is chosen, the statistics become dependent on the boundary choices, as explored in Christiansen (2005a).

To overcome this problem we use a flow-dependent latitudinal weighting of the geopotential height Z . The chosen weighting $w(\phi)$ as a function of latitude ϕ is proportional (the constant of proportionality is such that the latitudinal integral over w equals one) to the total variance of Z along the latitude circle:

$$w(\phi) \propto \int_0^{2\pi} [Z(\lambda, \phi) - \langle Z \rangle(\phi)]^2 \cos(\phi) d\lambda, \quad (3)$$

where $\langle Z \rangle$ is the zonal average of Z . This way the local wave amplitude is always evaluated at the latitudes where the waves are. The seasonal variation in jet location is automatically accounted for as well as decadal variability and secular trends in jet latitudes. Another advantage is that this weighting does not have any other parameters that may influence the statistics (although the power of the moment, in this case 2, could be considered a parameter). So, a latitudinal weighting as in Eq. (3) is defined and a longitudinally varying geopotential anomaly $f(\lambda)$ is found as

$$f(\lambda) = \int_0^{\pi/2} [Z(\lambda, \phi) - \langle Z \rangle(\phi)] w(\phi) d\phi. \quad (4)$$

This geopotential anomaly is then used to calculate the local wave amplitude from Eq. (1). An example can be found in Fig. 1 where strong Atlantic and Pacific blocks are clearly visible in the geopotential height field. The latitudinal weighting picks out the latitudes of the blocks and the resulting wave amplitudes pick out the longitudinal envelopes of the blocking waves with regions of relatively modest wave amplitude in between.

In summary, we have defined a local wave amplitude that generalizes the usual wave amplitude index by providing a consistent wave amplitude as a function of longitude and does not contain any tunable parameters. Because our local wave amplitude can be evaluated at any longitude of interest, independent of the phase of the carrier wave, and because it always takes into account the latitudes of interest, we expect this index to show real bimodality or multimodality if it is there in

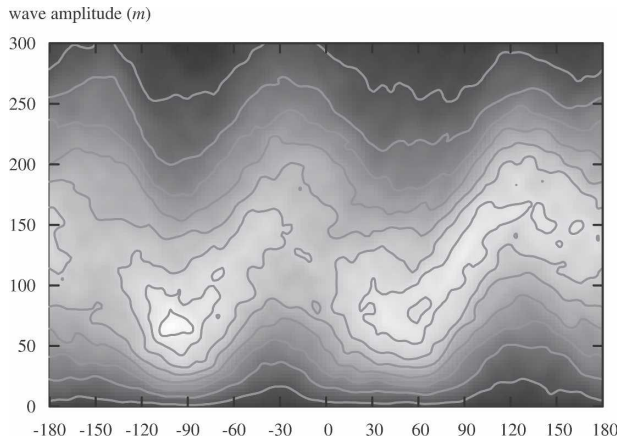


FIG. 2. Probability distribution function of the local wave amplitude of geopotential height at 500 hPa as a function of longitude. At each longitude the distribution function is normalized (i.e., integrates to one over amplitude). Four decades (1960–2000) of NDJFM low-pass filtered data are included.

the data. This is examined in detail in section 3. In section 4 the relationship between our local wave amplitude and the Hansen and Sutera wave amplitude index will be discussed.

3. Statistics of local wave amplitude

In this section we show some of the main observed statistics for the local wave amplitude, defined in the previous section. The data that we used are extracted from the 40-yr European Centre for Medium-Range Weather Forecasts (ECMWF) Re-Analysis (ERA-40) archive (Kållberg et al. 2005), enhanced with operational analyses of 6-hourly data for the four decades from 1960 to 2000. The data were low-pass filtered with a cutoff frequency of 10 days—we used a Lanczos filter with a length of 79 data points (20 days). The cutoff frequency was chosen to exclude synoptic activity from our amplitude index. A 5-day cutoff would perhaps be a more traditional choice, but in work with P. J. Athanasiadis (2008, unpublished manuscript), we show that variability is dominated by synoptic mobile systems at frequencies higher than 10 days. The 10-day cutoff is therefore a conservative choice to exclude these. We have recalculated the key statistics presented in Fig. 2 with a 5-day cutoff filter and found essentially the same results. The data were further limited to the months November–March (NDJFM), the meteorological winter period extended with adjacent months from the transitional seasons. As argued in the previous section, our local wave amplitude follows natural variations in latitudinal wave location, so there was no need to deseasonalize or detrend the data.

In Fig. 2 we present the empirical probability distribution function of the local wave amplitude as a function of longitude for all four decades. The overall structure shows peaks in average wave amplitude around 30°W and 140°E, the mid-Atlantic and west Pacific, respectively. For the mid-Atlantic this maximum amplitude presumably is associated with the strong variability of the Atlantic jet, also associated with the North Atlantic Oscillation. The west Pacific maximum is likely associated with the strong climatological trough over that area, which also registers as a high wave amplitude. The distribution function peaks at lower amplitude (and higher probabilities) around 90°W and 60°E. Although the distribution function has rich structure, there is no obvious strong sign of local bimodality.

It is not clear what theoretical distribution function the amplitude is expected to follow at each longitude. If the two contributions f and f^H to the amplitude in Eq. (1) were locally independent and had a Gaussian distribution with mean zero standard deviation σ , then the amplitude would follow a Rayleigh distribution, which is the same as a Weibull distribution with shape parameter $k = 2$ and scale parameter σ . In general, the Weibull distribution is defined as

$$g(A; \sigma, k) = \frac{1}{2} \frac{k}{\sigma} \left(\frac{A}{\sigma}\right)^{k-1} \exp\left[-\frac{1}{2} \left(\frac{A}{\sigma}\right)^k\right], \quad (5)$$

where σ is the scale parameter of the distribution and k the shape parameter. Given the weak a priori argument that the amplitude could follow a Rayleigh distribution, it makes sense to fit the empirical data to its generalization, a Weibull distribution.

Examples of such fits to a Weibull distribution are plotted in Fig. 3 (because of the high number of samples the fits were done as simple nonlinear curve fits). These fits show a range of shape parameters (1.8–3.0) and scale parameters. The longitudes in Fig. 3 are chosen to represent an extreme shape or scale parameter (see also Fig. 4). Longitudes around the Greenwich meridian (top right panel, Fig. 3) and 150°W (not shown) are unusual in that the amplitude distribution apparently has fairly substantial deviations from the fitted Weibull distributions, which could be candidates for multimodal distributions. However, for all other longitudes, the fit to the Weibull distribution is remarkably good.

The goodness of fit to the Weibull distributions was confirmed with a Kolmogorov–Smirnov test. For this test, the cumulative distribution of the observed data and of the fitted Weibull distribution are compared and tested for significance of any deviations. It was found that the null hypothesis, that the observed cumulative distribution was drawn from a fitted cumulative Weibull

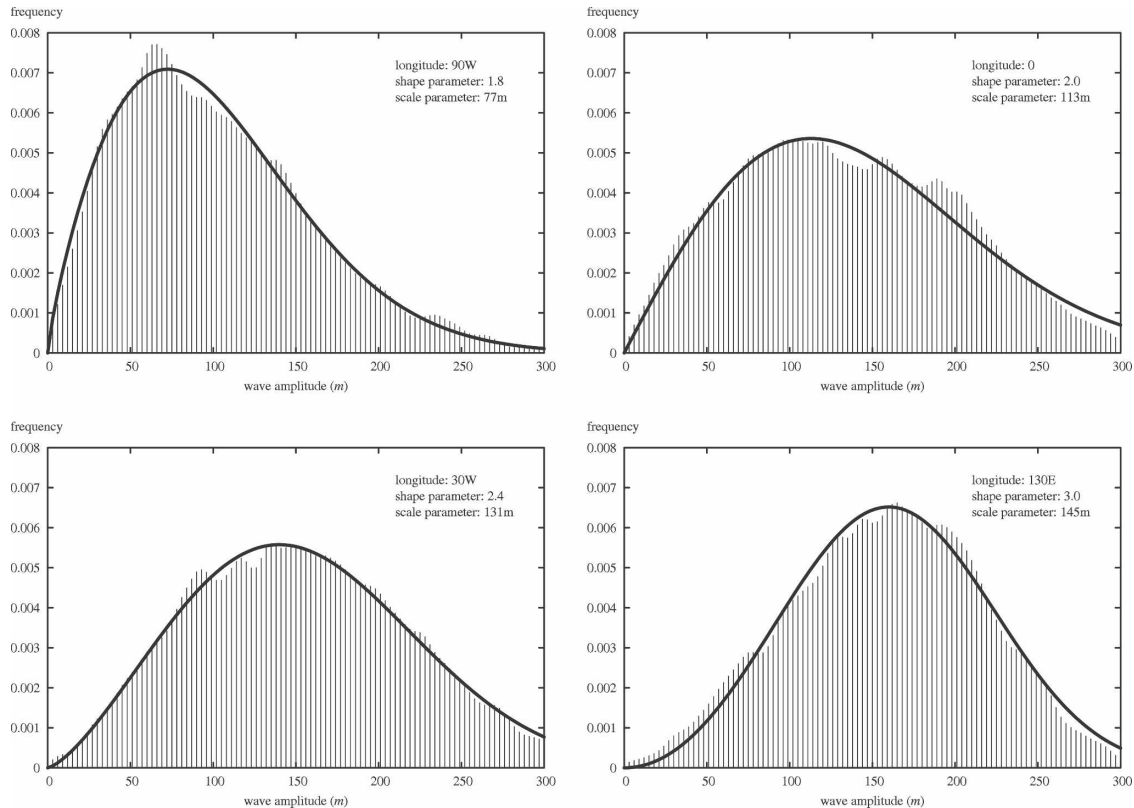


FIG. 3. Plots of Weibull distribution (thick line) fitted to the empirical distribution of wave amplitude (impulses) at four selected longitudes. Four decades (1960–2000) of NDJFM low-pass filtered data are included.

distribution, could not be rejected with a significance level better than 95%. Any significant deviations at selected locations or in selected decades could not be distinguished from sampling noise. The significance level is dependent on the number of chosen degrees of freedom. For our test, a single independent data point every 10 days was chosen, consistent with the low-pass filter time scale.

Figure 4 shows the shape and scale parameters for all longitudes of the fitted Weibull distributions. The stan-

dard errors (i.e., errors in the fitting of the parameters) have not been plotted since they are less than 1% for both parameters at all longitudes. The scale parameters clearly follow the dependency of the wave amplitude evident in Fig. 2. Perhaps surprisingly, the shape parameter also follows the variations of the scale parameter. The interpretation is that for locations for higher wave amplitudes the distribution does not simply scale up; it, in fact, moves away from zero amplitude (there are relatively fewer low amplitude cases). It can also be seen that the Rayleigh distribution (shape parameter of 2) is a fairly good model for the amplitude distribution for the longitudes of low average wave amplitude.

Figure 5 shows the empirical and fitted amplitude distributions at the Greenwich meridian for the four separate decades from 1960 to 2000. It is clear that the amplitude distribution has substantial interdecadal variability. Although this statistic is not directly comparable to the Hansen and Sutera wave amplitude index (see section 4 for a more detailed discussion), as in Christiansen’s (2005a) study, we find that 1990–2000 is the most perturbed decade, with a high shape parameter and high scale parameter for the fitted Weibull distribution. Especially in the period 1970–90 the em-

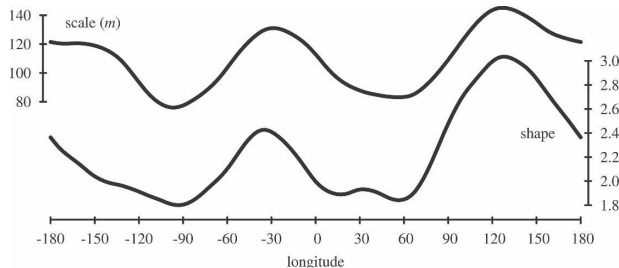


FIG. 4. Scale parameter (left ordinate) and shape parameter (right ordinate) of the Weibull distribution fitted to the empirical distribution of Fig. 2. Four decades (1960–2000) of NDJFM low-pass filtered data are included.

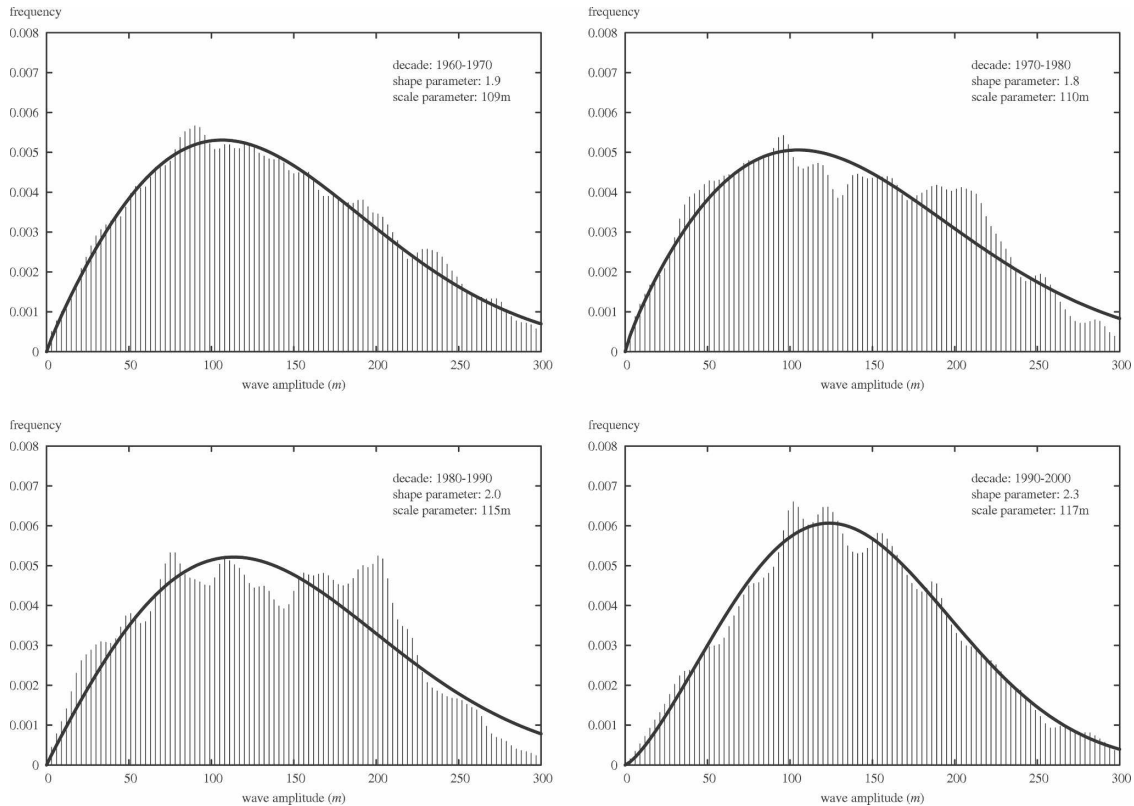


FIG. 5. Plots of Weibull distribution (thick line) fitted to the empirical distribution of wave amplitude (impulses) for the four separate decades at the Greenwich meridian.

pirical distribution appears remarkably broad that, in synoptic experience over those two decades, would certainly be experienced as a peculiar distribution: the near extremes are about as likely as the mean. Subtracting a smooth fitted distribution from the empirical distribution in these decades would give a bimodal anomaly structure. However, it could be argued that this is not really a relevant procedure to find bimodality; furthermore, based on the statistics alone, the peculiarity of the distribution at the Greenwich meridian in these decades would have to be interpreted as sampling variability.

4. Wave amplitude index and central limit theorem

We can define a wave amplitude index by integrating the squared amplitude A over longitude:

$$\begin{aligned} \text{WAI}^2 &= \int_0^{2\pi} A(\lambda)^2 d\lambda = \int_0^{2\pi} [f^2 + (f^H)^2] d\lambda \\ &= 2 \int_0^{2\pi} f^2 d\lambda. \end{aligned} \tag{6}$$

By Parseval’s theorem the zonal integral of f^2 equals the sum over the squared amplitudes of its Fourier components. Therefore, this definition becomes equivalent to Hansen and Sutera’s WAI if the signal was prefiltered to zonal wavenumbers 2–4 and the zonal anomaly f was defined over a fixed latitude belt. Following Eq. (2), the squared amplitudes of the Fourier components of the Hilbert transform are the same so that the total variance of the Hilbert transform is the same as the total variance of the original function, leading to the last equality in Eq. (6).

From our definition of the WAI it also becomes clear that our local wave can be interpreted as a generalized version of the WAI in that in addition to amplitude information it shows the phase information as well (i.e., at what longitudes waves interfere constructively to produce high local amplitudes).

Figure 6 shows the empirical distribution with a fitted normal distribution for our WAI defined over all four decades. A Weibull distribution did not fit the data (see below). The fitted normal distribution has a mean amplitude of 141(0.2) m and a standard deviation of 34(0.2) m. It is clear that the normal distribution fits the data very well. The empirical distribution has some

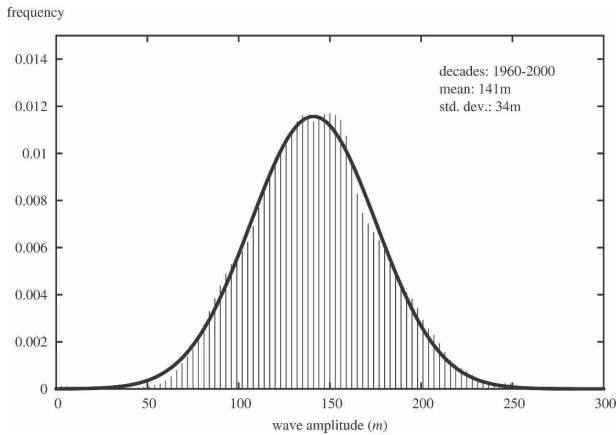


FIG. 6. The WAI as defined in Eq. (6) for the period 1960–2000 (impulses) with a fitted normal distribution (thick line).

structure near the peak but, even if it was statistically significant, there is no important multimodality.

Figure 7 shows our WAI over the different decades. Over all decades the Gaussian fit is good except for 1960–70. The clear bimodality for this decade was also observed by Hansen and Sutera (1986) and Christiansen (2005a; for a WAI also stratified according to

temporal rate of change). Quite apart from possible data issues for the presatellite era, this bimodality of the WAI turns out to be misleading. This becomes clear from Fig. 8, the empirical distribution of wave amplitude at each longitude for the 1960–70 decade. This figure is analogous to Fig. 7 with the phase information of each wave component retained. Note that no smoothing has been attempted, so most of the small-scale structure in Fig. 8 is sampling noise. However, it now becomes clear that the high amplitudes in Fig. 7 occur mainly at longitudes around 130°E, while the low amplitudes occur around 40°E and 90°W. There is no single longitude where the wave amplitude has a bimodal distribution as seen in the 1960–70 WAI. So the bimodality of the 1960–70 WAI does not represent local bimodality of the wave amplitude; it just represents the fact that different longitudes have, on average, either high or low wave amplitude with, in this decade, relatively few longitudes having an intermediate wave amplitude.

Next, we turn our attention to why the WAI appears to closely follow a normal distribution while the individual contributions are accurately modeled with Weibull distributions. First we determine how much the

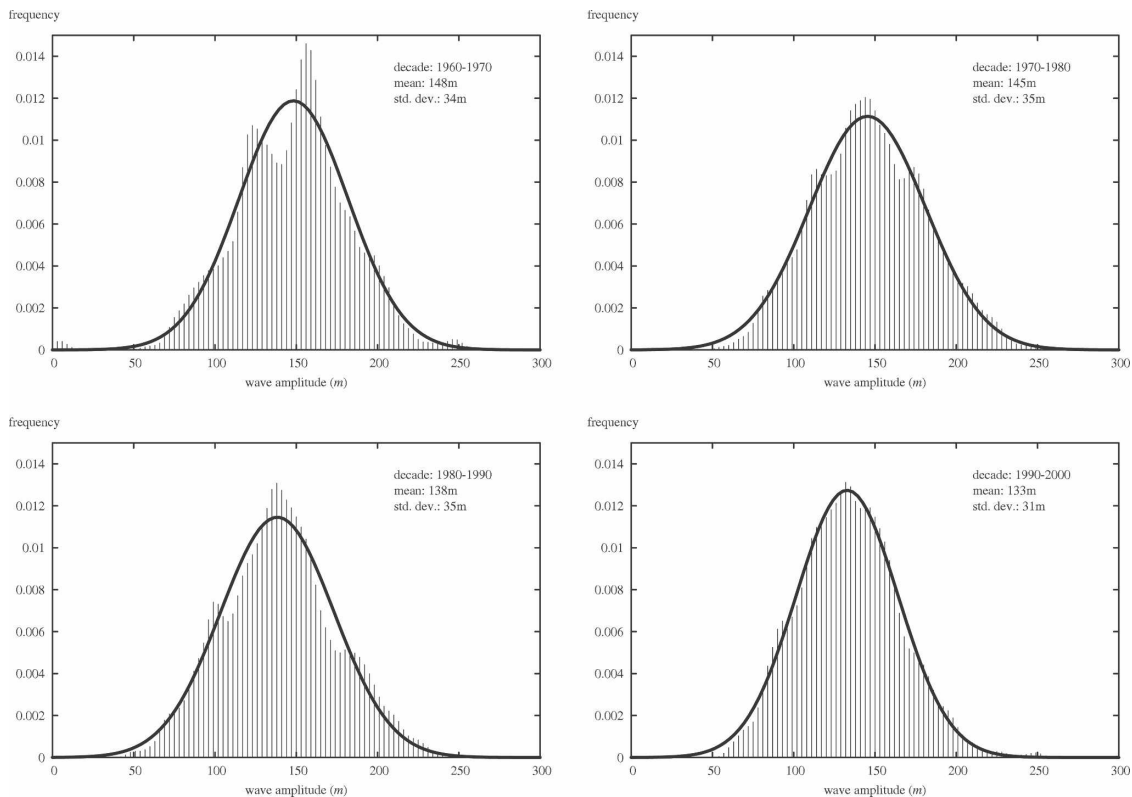


FIG. 7. The WAI as defined in Eq. (6) for the four different decades (impulses) with the fitted normal distributions (thick lines).

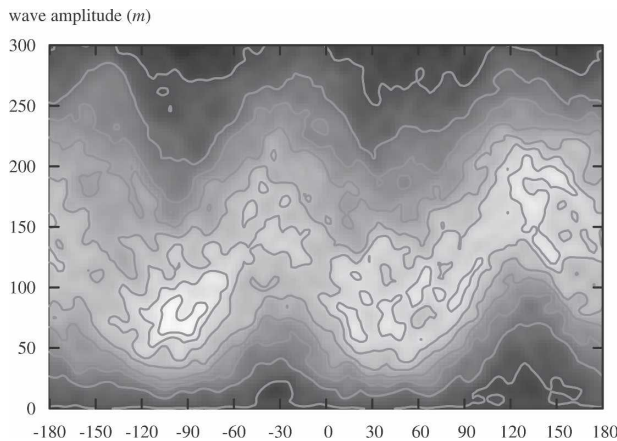


FIG. 8. Probability distribution function of the local wave amplitude of geopotential height at 500 hPa as a function of longitude. At each longitude the distribution function is normalized (i.e., integrates to one over amplitude). The decade 1960–70 of NDJFM low-pass filtered data is used.

integrands in the WAI [Eq. (6)] are independent. A good measure of how many independent data are to be found in the amplitude function is based on the autocorrelation. If the amplitudes $A(\lambda, t)$ are perfectly correlated between different longitudes, $r[A(\lambda_1), A(\lambda_2)] = 1$, then we have only one degree of freedom. If for each longitude combination for which $\lambda_1 \neq \lambda_2$ we have $r[A(\lambda_1), A(\lambda_2)] = 0$, then the number of degrees of freedom is (at least) the number of grid points in the longitude direction. For intermediate values of the autocorrelation scale we can estimate the number of degrees of freedom M as

$$\frac{1}{M} = \left\langle \frac{1}{N} \sum_{i=1}^N r[A(\lambda_i), A(\lambda_i)] \right\rangle, \quad (7)$$

where N is the number of grid points and $\langle \cdot \cdot \rangle$ denotes an average over longitudes λ_i . Using this measure we find around 3.6 degrees of freedom (the number of degrees of freedom is usually thought of as an integer, but in many applications there is no problem in generalizing this to a fractional number) with the spatial decay scale of the autocorrelation of the wave amplitude at about 50° of longitude (the wave amplitude envelope in Fig. 1 should be interpreted in this light). So, our WAI index is made up of the sum of 3.6 independent variables. The set of empirical distributions at each longitude does satisfy the Lindeberg conditions on the central limit theorem for variable distributions (e.g., Feller 1968). This then means that our WAI *by definition* will look similar to a Gaussian distribution. Clearly, with only 3.6 degrees of freedom the limit to the Gaussian distribution is not complete. However, the convergence

to the limit is generally very swift (also evidenced by how far the empirical distribution functions in Figs. 6 and 7 are from a Weibull distribution), so our WAI is bound to be close to having a Gaussian distribution.

The application of the central limit theorem to our WAI clearly has profound consequences for its use in detection of multimodality: even if the atmosphere had multimodality at particular (or all) longitudes and if the amplitude between longitudes decorrelates sufficiently fast, the central limit theorem implies that the WAI index will be normally distributed. Under these circumstances the WAI is unsuitable to detect multimodality. Any observed multimodality will be the result of sampling errors or unstable statistics.

5. Summary and discussion

A measure of local (in longitude) wave amplitude has been introduced. A consistent amplitude is defined at each longitude using spatial Hilbert transforms to extract a wave envelope. The wave is a latitudinally weighted geopotential height anomaly at 500 hPa. The latitudinal weighting is proportional to the wave variance at each latitude.

At all longitudes the local wave amplitudes appear to follow Weibull distributions with shape parameters between about 2 and 3 and scale parameters between 100 and 140 m. The shape parameter turns out to be high where the amplitude is high, indicating that in regions of high average amplitudes the low amplitudes are relatively underrepresented. At the tail ends of the Pacific and Atlantic storm tracks the empirical distributions are relatively farthest away from the fitted Weibull distributions, although the hypothesis that those distributions are drawn from a Weibull distribution cannot be rejected at the 95% significance level.

The empirical distributions have substantial decadal variability. For example, in the 1970–90 period the wave amplitude at the Greenwich meridian has a flat distribution between amplitudes of about 50 and 250 m. Although this is largely averaged out over the four-decade period, it clearly represents a substantial period with unusual statistics. During this 20-yr period there is an unexpectedly high probability of finding either relatively high or low amplitudes. It is a subject of future study to determine whether this is the result of weather regime residence times. Any conceptual model for this result should be able to explain why the other two decades apparently do not show these unusual statistics.

The local amplitude can be integrated over longitude to provide a hemispheric wave amplitude index, similar to Hansen and Sutera's (1986) WAI. It is shown that for the full data period under consideration the WAI is

close to a normal distribution. Again, there is substantial decadal sampling variability with the 1960–70 decade showing a bimodal distribution. However, it is shown that the high and low amplitude states of this distribution are, in fact, realized at different longitudes, thus showing no real bimodality at any longitude in that decade.

Note that our WAI values are higher by a factor of 2 than those found in previous studies because we included the variance of the Hilbert transform as well [Eq. (6)]; the choices of a temporal filter (10-day low pass compared to 5 day), latitudinal weighting (variance weighting compared to a fixed latitude belt), and the included longitudinal wavenumbers (all waves compared to wavenumbers 2–4) do not introduce large changes in mean wave amplitude. The inclusion of the higher-longitudinal wavenumbers has only modest influence because of the temporal filtering. It is perhaps more surprising that the latitudinal variance weighting has so little influence on the mean amplitude. Apparently the variance weighting simply provides a consistent way of locating the latitudes of interest.

With the WAI as the integral of local wave amplitudes, the central limit theorem can be applied to it, insofar as different longitudes are independent. It is shown that the local wave amplitude contains 3 to 4 independent degrees of freedom. This means that the limit to the Gaussian distribution is not complete. However, the convergence is strong enough to generally prevent the appearance of bimodality, even if bimodality was clear in the local data and if the data record was long enough to prevent sampling errors. It is also expected that the time filtering of the data increases the longitudinal autocorrelation scale and so reduces the effective number of degrees of freedom. Unfiltered data are therefore expected to show an even more Gaussian WAI.

Methods of looking at distributions in two-dimensional projections of the atmospheric phase space usually employ empirical orthogonal functions (EOFs) or some other spatial pattern to span the two-dimensional projection space. Such methods also potentially suffer from the strong convergence of the central limit theorem.¹ For example, an empirical orthogonal function is a spatial pattern that, in general, can cover uncorrelated (linearly independent) locations (e.g., Ambaum et al. 2001). This means that the corresponding time series is

a weighted sum of independent variables and by the central limit theorem will have Gaussian statistics. The time series probably contains only few independent variables so the limit is certainly incomplete, but the convergence to a Gaussian distribution is remarkably fast. Under such circumstances it will, by definition, be impossible to see more structure in the combined empirical distribution function other than a bivariate approximate Gaussian distribution. Clearly, if it can be shown that any principal component time series truly represents a single atmospheric degree of freedom [this would, e.g., be more likely for stratospheric EOFs; see, e.g., Christiansen (2003)], then it will be possible to find non-Gaussian structure, if the underlying atmospheric data were non-Gaussian. But by virtue of the central limit theorem, such EOFs need to represent strong teleconnectivity and cannot contain several independent signals.

Acknowledgments. This work benefited from discussions with David Straus, David Stephenson, and Brian Hoskins. Bo Christiansen and an anonymous reviewer are thanked for their insightful comments on an earlier version of the manuscript.

REFERENCES

- Ambaum, M. H. P., 1997: Large-scale dynamics of the tropopause. Ph.D. thesis, Eindhoven University of Technology, 128 pp.
- , and W. T. M. Verkley, 1995: Orography in a contour dynamics model of large-scale atmospheric flow. *J. Atmos. Sci.*, **52**, 2643–2662.
- , and P. J. Athanasiadis, 2007: The response of a uniform horizontal temperature gradient to heating. *J. Atmos. Sci.*, **64**, 3708–3716.
- , B. J. Hoskins, and D. B. Stephenson, 2001: Arctic Oscillation or North Atlantic Oscillation? *J. Climate*, **14**, 3495–3507.
- Branstator, G., and J. D. Opsteegh, 1989: Free solutions of the barotropic vorticity equation. *J. Atmos. Sci.*, **46**, 1799–1814.
- Charney, J. G., and J. G. DeVore, 1979: Multiple flow equilibria in the atmosphere and blocking. *J. Atmos. Sci.*, **36**, 1205–1216.
- Christiansen, B., 2003: Evidence for nonlinear climate change: Two stratospheric regimes and a regime shift. *J. Climate*, **16**, 3681–3690.
- , 2005a: Bimodality of the planetary-scale atmospheric wave amplitude index. *J. Atmos. Sci.*, **62**, 2528–2541.
- , 2005b: The shortcomings of nonlinear principal component analysis in identifying circulation regimes. *J. Climate*, **18**, 4814–4823.
- Corti, S., F. Molteni, and T. N. Palmer, 1999: Signature of recent climate change in frequencies of natural atmospheric circulation regimes. *Nature*, **398**, 799–802.
- Ek, N. R., and G. E. Swaters, 1994: Geostrophic scatter diagrams and the application of quasigeostrophic free-mode theory to a northeast Pacific blocking episode. *J. Atmos. Sci.*, **51**, 563–581.
- Feller, W., 1968: *An Introduction to Probability Theory and Its Applications*. 3rd ed. John Wiley & Sons, 509 pp.

¹ Jolliffe (2002) and Stephenson et al. (2004) have previously referred to such a property of EOFs, however ignoring the essential role of (partial) independence of the loading vectors. EOFs do not by definition produce Gaussian time series since they could in principle reflect a single, multimodal physical mechanism.

- Flierl, G. R., 1987: Isolated eddy models in geophysics. *Annu. Rev. Fluid Mech.*, **19**, 493–530.
- Hansen, A. R., and A. Sutera, 1986: On the probability density distribution of planetary-scale atmospheric wave amplitude. *J. Atmos. Sci.*, **43**, 3250–3265.
- Jolliffe, I. T., 2002: *Principal Component Analysis*. 2nd ed. Springer, 487 pp.
- Kållberg, P., P. Berrisford, B. J. Hoskins, A. Simmons, S. Uppala, S. Lamy-Thépaut, and R. Hine, 2005: ERA-40 Atlas. ERA-40 Project Rep. Series 19, 191 pp.
- Kimoto, M., and M. Ghil, 1993: Multiple flow regimes in the Northern Hemisphere winter. Part I: Methodology and hemispheric regimes. *J. Atmos. Sci.*, **50**, 2625–2644.
- Malguzzi, P., and A. Speranza, 1981: Local multiple equilibria and regional atmospheric blocking. *J. Atmos. Sci.*, **38**, 1939–1948.
- McWilliams, J. C., 1980: An application of equivalent modons to atmospheric blocking. *Dyn. Atmos. Oceans*, **5**, 43–66.
- Mo, K., and M. Ghil, 1988: Cluster analysis of multiple planetary flow regimes. *J. Geophys. Res.*, **93**, 10 927–10 952.
- Monahan, A. H., L. Pandolfo, and J. C. Fyfe, 2001: The preferred structure of variability of the Northern Hemisphere atmospheric circulation. *Geophys. Res. Lett.*, **28**, 1019–1022.
- Nitsche, G., J. M. Wallace, and C. Kooperberg, 1994: Is there evidence of multiple equilibria in planetary wave amplitude statistics? *J. Atmos. Sci.*, **51**, 314–322.
- Palmer, T. N., 1999: A nonlinear dynamical perspective on climate prediction. *J. Climate*, **12**, 575–591.
- Stan, C., and D. M. Straus, 2007: Is blocking a circulation regime? *Mon. Wea. Rev.*, **135**, 2406–2413.
- Stephenson, D. B., A. Hannachi, and A. O'Neill, 2004: On the existence of multiple climate regimes. *Quart. J. Roy. Meteor. Soc.*, **130**, 583–605.
- Swanson, K. L., 2002: Dynamical aspects of extratropical tropospheric low-frequency variability. *J. Climate*, **15**, 2145–2162.
- Tung, K. K., and A. J. Rosenthal, 1985: Theories of multiple equilibria—A critical reexamination. Part I: Barotropic models. *J. Atmos. Sci.*, **42**, 2804–2819.
- Verkley, W. T. M., 1984: The construction of barotropic modons on a sphere. *J. Atmos. Sci.*, **41**, 2492–2504.
- von Storch, H., and F. W. Zwiers, 1999: *Statistical Analysis in Climate Research*. Cambridge University Press, 484 pp.
- Zimin, A. V., I. Szunyogh, D. J. Patil, B. R. Hunt, and E. Ott, 2003: Extracting envelopes of Rossby wave packets. *Mon. Wea. Rev.*, **131**, 1011–1017.